Green Polymer Nanocomposites: Formation via Plastic Deformation, Structure, Properties and New Application Opportunities

Andrey Voznyak, Alina Vozniak, Yuliia Goriainova
Donetsk National University of Economics and Trade
named after M. Tugan-Baranovsky,
Krivoy Rog, Ukraine

Yurij Voznyak
Polymer Physics Department
Centre of Molecular and Macromolecular Studies, Polish
Academy of Sciences,
Lodz, Poland

***Abstract*—Through the example of polylactide (PLA) and poly (1,4-butylene succinate) (PBS), the possibility of making sustainable "green nanocomposites" by slit die extrusion process in a single screw extruder has been investigated. The main feature of the received structures is the formation of stable shear bands. Their role in the crazing development and their mutual interaction under uniaxial tension for PLA and PLA/PBS composite was investigated by in-situ tensile testing in the SEM experiments. It has been established that pre-existing shear bands contributes to ductility by blocking and diffusing standard craze growth. Moreover, PBS nanofibers, formed by extrusion, additionally confer to ductile character of PLA/PBS composites by providing pre-existing shear bands and craze rotation. Tensile experiments revealed an essential growth of ductility and retaining of high strength and stiffness of the extruded PLA and PLA/PBS composite.**

Keywords—biocomposite; nano-structures; fibres; plastic deformation; electron microscopy; extrusion

I. INTRODUCTION

Due to increasing awareness about the global environment a range of new polymeric materials is being developed, especially biodegradable materials and those produced from renewable resources. Contrary to conventional polymers, biodegradable polymers can be converted into biomass or into carbon dioxide and water. Biopolymer blends market shares its continuous growth. It is widely known that the use of several polymers combined in a blend allows obtaining several advantages, in particular, a combination of the best of their properties. It is known that the performance of polymer blends not only depend on the physical characteristics of its components, but also highly on the phase interface. In theory, blends of polymers can assume required properties when mixed in different proportions. However, blends with phase separation usually display poor physical and mechanical properties. In order to improve compatibility and performance of polymer blends, several methods are applied including the use of a compatibilizer, chemical grafting, coupling, or physical modification etc [1–6].

The degree of adhesion between the filler and the matrix depends both on the individual properties of the two components and the size, shape, and state of agglomeration of the minor component. For the sake of convenience, one may differentiate fillers into two main groups: particulate and fibrous. Particulate phases are usually called fillers, or if the interphase adhesion is high, reinforcing fillers. Fibrous phases are usually referred to as reinforcing, for the fibers themselves bear an important fraction of any load applied.

As a rule, particulate fillers tend to increase the stiffness of a polymer matrix but may or may not increase the toughness or tensile strength, depending on the ductility of the matrix and the degree of filler-matrix adhesion. In many cases, the toughness is in fact decreased by spherical or substantially isometric particles, especially if good filler-matrix adhesion exists. On the other hand, even short fibers often confer quite synergistic mechanical properties, such as a combination of high modulus, strength, and toughness.

Thus, the achievement of high performance of polymer blends is highly expected, mainly derived from stiff extended nanofibrils and enhanced interfacial interactions. In the present research, this fact was reached by conversion of polymer blends into *in situ* composites, instead of adding ready-made fibers.

The nanofibers of one polymer will be formed inside the second polymer during shear processing in a melt. The solidification of nanofibrous sheared inclusions will be instantaneous due to shear induced crystallization, all during processing. This concept will allow formation of "all-polymer" nanocomposites in a single step.

II. EXPERIMENTAL

A. Materials

PLA 4060D purchased from NatureWorks LLC (Minnetonka, MN), with density of 1.24 g cm^{-3}, weight average molar mass Mw of 120 kg mol−1 and polydispersity Mw/Mn=1.4 as determined by size exclusion chromatography (SEC) with multi-angle laser light scattering detector in dichloromethane. D-Lactide and L-lactide contents were 18 and 82 mol%, respectively, as determined by measurements of specific optical rotation. The presence of 18% DLA prevented PLA from crystallization during thermal treatment. Poly (1,4-butylene succinate), extended with 1,6-diisocyanatohexane was a commercial product purchased from Sigma-Aldrich

(USA) Co., Ltd. It shows a melting point of 120 °C and a melt flow index of 10 g/10 min (190 °C/2.16 kg, ASTM D1238).

B. Sample preparation

To avoid the degradation due to hydrolysis and prevent the formation of voids during processing, biopolymers were dried for 24 h at 40 °C under vacuum overnight before extrusion. Melt blending of biopolymers will be carried out in a co-rotating twin screw extruder with a ratio of screw length to its diameter (L/D) of 40. Further blending will be followed by extrusion of tapes using single screw extruder (L/D = 25) equipped with the 12 mm wide, 0.8 mm thick and 100 mm long slit die. Temperatures in the zones were 170, 150, and 135 °C from the feed section to the die, respectively. The slit die process parameters were as follows: temperature - 130 °C, pressure – 65.0 MPa. The extrudates were cast on a transport belt at T = 25 °C). The extrudates in the form of tapes approximately 0.75 mm thick and 10 mm wide were obtained. Neat PLA was also processed under the same condition to obtain a reference material. For examination of the properties of initial PLA and PLA/PBS composite 0.75 mm thick films of the materials were compression molded at 170 °C for 3 min, and quenched between thick metal blocks kept at room temperature.

C. Sample characterisation

Rheological measurements were performed to determine the rheological behavior of extruded blends, taking advantage of a parallel-plate geometry with a diameter of 20 mm. The small amplitude oscillatory shear (SAOS) was applied in all dynamic measurements. The sheet samples were melted to eliminate the residual thermal histories, and the dynamic frequency sweep will be then carried out immediately. In other experiments the melting temperature will be low enough not to melt nanofibers of the other polymer. A common strain level fixed at 10% will be predetermined by the dynamic strain sweep.

2D-WAXD determination was employed to evaluate molecular orientation and crystalline morphology of fibrillar composites. 2-D WAXS images were registered with flat X-Ray camera equipped with imaging plates (Fuji) and coupled to Cu Kα source (sealed tube operating at 30 kV and 50 mA, Philips). In addition the x-ray measurements were performed with a diffractometer attached to Philips sealed tube x-ray source set in the reflection mode.

Differential scanning calorimeter (DSC) was used to probe the thermal features such as glass transition, melting and crystallization behaviors for pure polymers and fibrillar composites. Thermal behavior of samples was probed with DSC 2920 differential scanning calorimeter (TA Instruments) during heating from -50 °C to 190 °C with the rate of 10 °C /min. Samples of the 7–8 mg mass were cut out from extruded PLA and PLA/PBS composites and crimped in standard Al pans. The DSC cell was purged with dry nitrogen during the measurements (20 ml/min).

SEM was employed to observe the phase morphology, fibrillar structure, and crystalline morphology. Cryogenic fracture and selective etching were applied to obtain the specific surfaces.

Tensile deformation was investigated by *in-situ* experiments in SEM chamber using Gathan stress strain device that can fit to the SEM Jeol 5010LV sample chamber. Sample for such studies were sputtered with carbon. The specimen for *in-situ* SEM observation were prepared according to the ASTM standard D638. Oar-shaped specimens, with the gauge length of 9.53 mm and the width of 3.18 mm, were cut out from the compression molded films and from extruded tapes using a steel template. *In-situ* observations of tensile experiments were conducted in a JEOL JSM-5500 LV scanning electron microscope with a Gatan MT200 microtest tensile stage with maximum load capacity of 200 N at room temperature using an accelerating voltage of 15 kV. The deformation rate of the microtest was 0.2 mm/min. During tensile process, at some strain points, the tensile process was paused and the load was held, and then SEM images were taken. It should be pointed out that a slight stress relaxation occurred during the pauses. After SEM images were taken, the tensile process was continued.

The tensile properties were also measured using large size machine (“Instron”) and mini stretcher, constructed by “Linkam”, allowing to perform tensile deformation in a wide temperature range. Tensile measurements were performed according to the ISO 527-2 standard. Specimens of the gauge length of 25 mm and the width of 5 mm (ISO 527-2, type 1BA) were cut out from the compression molded films and from extruded tapes using a steel template. For extrudates specimens oriented along the extrusion directions were prepared.

Shear-induced crystallization of the polymer inclusions was carried out in the Linkam optical shearing system CSS450. The specimens were subsequently subjected to the corresponding thermomechanical treatments. Control specimens were nonisothermally crystallized without pre crystallization shearing. The initial PBS films were prepared by compression molding at 170° C for 3 min and quenching to room temperature. The specimens were subsequently subjected to the following thermomechanical treatment: 1. heating to 150 °C at 30 °C min^{-1}, 2. holding at 150 °C for 3min to erase some possible orientation of polymer, 3. cooling down at 20 °C min^{-1} to temperature (T_f) with simultaneous shearing at a rate ranging from 300 to 1000 s^{-1}, 4. cooling at 20 °C min^{-1} to room temperature. Control specimens was nonisothermally crystallized without pre-crystallization shearing. The entire thermal treatment was conducted under a nitrogen flow.

III. RESULTS AND DISCUSSION

According to the tensile test it was shown that in the initial PLA brittle fracture is observed in the apparent elastic region, below the macroscopic yield stress. For the PLA processed by extrusion a neck appears after yielding. Extrusion of PLA results also in an increase in the Young modulus, the yield stress and the stress at break with respect to initial PLA. Strain at break of the extruded PLA was higher than that of the initial PLA. Thus, it was shown that, two distinct mechanical behavior of PLA are evidenced. On the one hand, for

Td=22 °C, initial PLA exhibits a brittle behavior. On the other hand, for Td=22 °C, extruded PLA exhibits a ductile behavior. Therefore, it appears that due to the extrusion a brittle to ductile transition occurs. Such transition was also observed for PLA upon increasing the draw temperature (just below or close to glass transition temperature T_g) in the tensile test [7]. It is known that in the case of amorphous polymers [as well as crystalline polymers these the brittle to ductile transition originates from the change from crazing to shear-banding.

Adding 3wt.% of the PBS into PLA results in a minor decrease in Young modulus from 2.04 GPa to 1.83 GPa and moderate decrease of the stress at break from 43 MPa to 38.2 MPa. Strain at break of the PLA/PBS composite was higher than that of the neat PLA (7.8% vs. 7.0%). At the same time, extrusion created an increase in strain at break up to 17.2% and 70% for neat PLA and PLA/PBS composite, respectively. Moreover, the extrusion also causes a slight increase of Young modulus to 2.11 GPa (PLA) and 2.19 GPa (PLA/PBS). However, the yield stress and the stress at break (38.0 MPa and 36.0 MPa in the case of extruded PLA and 36.0 MPa and 33.1 MPa for extruded PLA/PBS) were slightly lower than for neat PLA and PLA/PBS composite.

In-situ tensile testing in the SEM revealed that initial PLA demonstrates a quite brittle fracture with severe localization of strain before yielding. This is caused by craze nucleating before the yielding and subsequent rapid craze-crack transition. In this case small amount of crazes appeared and therefore fibrils to contribute to the load-bearing capacity. Sample failure occurs as soon as the fibrils reach their critical elongation, i.e. when yield stress becomes higher than the critical stress for fibril breakdown.

In the case of extruded PLA initial microstructure consists of uniformly distributed shear bands. Up to the yield point any visible changes in the shear structures of both types of PLA are not observed. Then, beyond the yield point, crazes are generated and propagate perpendicular to the main stretch direction. With the increase of strain the crazes are becoming much more numerous. However, the dormant shear bands contributes to the overall deformation. Crazes tend to coalescent in a broad deformation zone where dense and deflected crazes start to merge to form a deformation band. Crazes once formed they retain their thickness. With further deformation new crazes are formed and eventually transform into a macroscopic neck. Dormant shear bands mainly deflect, blunt and terminate crazes, and are helpful in initiation of new crazes. It should be noted that the effect of shear bands substantially limits to the inhibition or initiation of craze development. During further deformation their multiplication takes place. Dormant shear bands may stop the propagation of the crazes and stabilize them. In addition, shear bands can act as preferential nucleation sites for crazes.

PBS and polyhydroxyalkanoate (PHA) showed the increase in non isothermal peak crystallization temperature by 30 °C and 50 °C, respectively. In accordance with our expectations, it appeared that the orientation stretching of the inclusions results in formation of nanofibrils. The extruded tape of PLA/PBS blend contained many long fibrillar inclusions of PBS as it is seen in Fig. 1 where SEM image of surface etched extruded tape is presented. Sodium hydroxide etching preferentially targeted towards PLA leaving nearly intact PBS.In particular, PBS fibers are of the thickness in the range from 30 to 100 nm and their length is in the range of 5–10 μm. It is seen that the fibrils are uniformly distributed over the volume of the polymer matrix, being rigorously aligned with the direction of stretching. These results are exciting and promising for other polymer system as well.

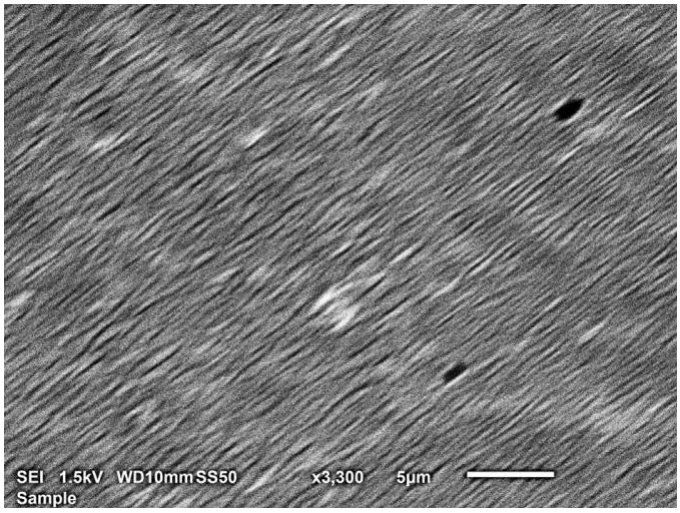

Fig. 1. Morphology of PLA/PBS extruded composite exposed by selective etching

Preliminary study has demonstrated that the modification of the matrix plays also a significant role in formation of improved set of properties. In particular, in the PLA-PBS blend, it is shown that the conditions of conversion into *in situ* composites (high shear rate and the extrusion temperature) provide formation of shear bands in the structure of polymer matrix. As a result, due to the interaction of crazes and shear bands, the ductility of the polymer blend increases almost tenfold (or by an order), with the transition from brittle fracture to ductile one determined. It should be noted that a contribution is also made by enhanced interfacial interactions. In particular, it was found that PBS nanofibers were spanning PLA craze surfaces and bridging craze gaps when PLA nanofibrils broke at large strain.Unprecedented results consisting in simultaneous increase in ductility and retaining rigidity were caused by the formation of shear bands in PLA as well as the generation of PBS nanofibers. The PBS nanofibers aside from strengthening acted as effective spanning of PLA craze surfaces, reinforcing the crazes. All these was achieved at only 3wt.% of PBS in PLA, in contrast to 40 wt.% of PBS as used by Hsia et. Al. [8]. It should be noted that polymer nanocomposites contain substantially less filler (1-5 vol.%) and thus enabling greater retention of the inherent processability and toughness of the neat polymer matrix.

The extent of the loss of fiber's strength and stiffness depends on the aging time and temperature. It has been recently clarified that there are three flow regimes in shear-induced crystallization of polymers. Meerveld et al. [9] have shown that for shear rates lower then $1/\tau d$, where τd is the

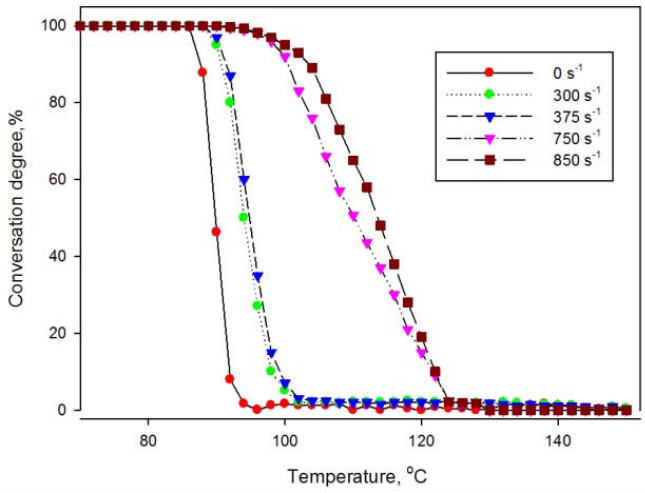

Fig. 2. Dependencies of conversion degree of PBS during cooling with the rate 20 °C/min from 150 °C with simultaneous shearing with various shearing rates

reptation or disentanglement time, no noticeable influence of the shear flow is observed, so, crystallization occurs as for quiescent conditions. For this regime the related Weissenberg numbers, defined as Wio = $\tau d\ \gamma$ (related to molecular orientation) and Wis = $\tau R\ \gamma$, where τR is the Rouse time (related to molecular stretch), are both smaller than 1, i.e. Wio < 1, Wis < 1. If shear rate is higher than $1/\tau d$, but lower then $1/\tau R$, only orientation effects enhance the point nucleation. This leads to a more fine grained but still spherulitic morphology. For the Weissenberg numbers it now holds: Wio ≥ 1, Wis < 1. Finally, if shear rate higher then $1/\tau d$ and $1/\tau R$ molecular stretch ccurs and the flow generates oriented shish-kebabs structures, that is, fibrillar nuclei (shish), on which lamellae grow aterally (kebabs). For the Weissenberg numbers it now holds: Wio ≥ 1, Wis ≥ 1. Thus, depending on the melt flow strength, expressed in terms of different characteristic time scales, the different number and length of extra nuclei as well as different morphology types are possible. So, it is very important to perform the crystallization of *in-situ* formed nanofibers as fast as possible and at the temperature close to the peak crystallization temperature. We expect that shearing in the extruder with shear rates between 200 and 700 s^{-1} (calculated using extruder parameters: screw diameter, screw rotation speed and clearance between screw and cylinder wall) and directing the sheared material into a slot capillary will lead to strong elongation of PBS inclusions into fibers, especially when the temperature at the capillary is strongly reduced. The fibers will crystallize at 20-30 °C higher temperature than at the quiescent state because of the influence of shear rate. Crystallization will stabilize the elongated shape and molecular orientation of PBS fibers during further processing and quenching of the PLA matrix. The material when passing from the compounding zone of the extruder (with high shear rate and high temperature) to slot capillary zone undergoes severe elongational deformation. The deformation exceeds 30 times as it can be estimated from the ratio of cross-sections: compounding zone having 300 mm^2 ($\pi D^2/4$) while slot capillary zone only 0.96 mm^2 (H*B=0.8 mm*12 mm) and causes the formation of extremely extended PBS fibres embedded in PLA matrix. Sheared and elongated material enters the slot capillary zone where the temperature is much lower (130 °C) and PBS fibers start to solidify by shear and elongation stimulated crystallization.

For this purpose, the study will consider the concept of lowered temperature in the slot capillary. The method allows shifting of the non-isothermal crystallization peak temperature of polymer inclusion by 20-50 °C towards higher temperatures by increasing the shear rate. Fig.2 illustrates the temperature dependencies of conversion degree of PBS during cooling with simultaneous shearing with various shearing rates.

ACKNOWLEDGMENT

The project was financed from funds of the State Fund For Fundamental Research (project N F71/61-2017).

REFERENCES

[1] J.L. White and S.H. Bumm, "Polymer blend compounding and processing," in Encyclopedia of Polymer Blends, A.I. Isayev and S. Palsule, Eds. Germany: Wiley-VCH, 2011.

[2] Y. Wang and L. Zhang, "Blends and Composites Based on Cellulose and Natural Polymers," Chapter 6 in Biodegradable Polymer Blends and Composites from Renewable Resources, L. Yu, Ed. New Jersey: John Wiley & Sons, Inc., 2008.

[3] C.C. Chen and J.L. White, "Compatibilizing agents in polymer blends: Interfacial tension, phase morphology, and mechanical properties," Polym. Eng. Sci., vol. 33, pp. 923–930, 1993.

[4] S.H. Anastasiadis, "Interfacial tension in binary polymer blends and the effects of copolymers as emulsifying agents," Adv. Polym. Sci., vol. 238, pp. 179-187, 2011.

[5] H.B. Eitouni and N.P. Balsara, "Thermodynamics of polymer blends," Chapter 19 in Physical Properties of Polymers Handbook, 2nd ed., J.E. Mark, Ed. New York: Springer, 2007.

[6] P.C. Painter and M.M. Coleman, "Hydrogen bonding systems," Chapter 4 in Polymer Blends, D.R. Paul and C.B. Bucknall, Eds. New York: Wiley, 2000.

[7] G. Stoclet, J.M. Lefebvre, R. Séguéla, and C. Vanmansart, "In-situ SAXS study of the plastic deformation behavior of polylactide upon cold-drawing," Polymer, vol. 55, no. 7, pp. 1817-28, 2014.

[8] L. Xie, H. Xu, B. Niu, X. Ji, J. Chen, Z.M. Li, B.S. Hsiao, and G.J. Zhong, "Unprecedented Access to Strong and Ductile Poly(lactic acid) by Introducing In Situ Nanofibrillar Poly(butylene succinate) for Green Packaging," Biomacromolecules, vol. 15, pp. 4054-4064, 2014.

[9] J.Van Meerveld, G.W.M. Peters, M. Hutter, "Towards a rheological classification of flow induced crystallization experiments of polymer melts," Rheol. Acta, vol. 44, no. 2, pp. 119-134, 2004.